Sogang University
SMOS Laboratory

Weekly Meeting
Journal Club

Fourier-transform sum-frequency surface vibrational spectroscopy with femtosecond pulses

J. A. McGuire, W. Beck, X. Wei, and Y. R. Shen

Department of Physics, University of California, and Materials and Chemical Sciences Division, Lawrence Berkeley Laboratory, Berkeley, California 94720

Received August 9, 1999

We present a Fourier-transform spectroscopic technique for investigation of surfaces and interfaces based on IR–visible sum-frequency generation with femtosecond light pulses. The observed spectrum has a resolution that is independent of the input pulse characteristics.

OCIS codes: 190.4350, 300.6300, 190.7110, 300.6490.

Presenter: Krem Sona
09-September-2017

Introduction

Under electric dipole approximation, SFG cannot be observed in centrosymmetric media.

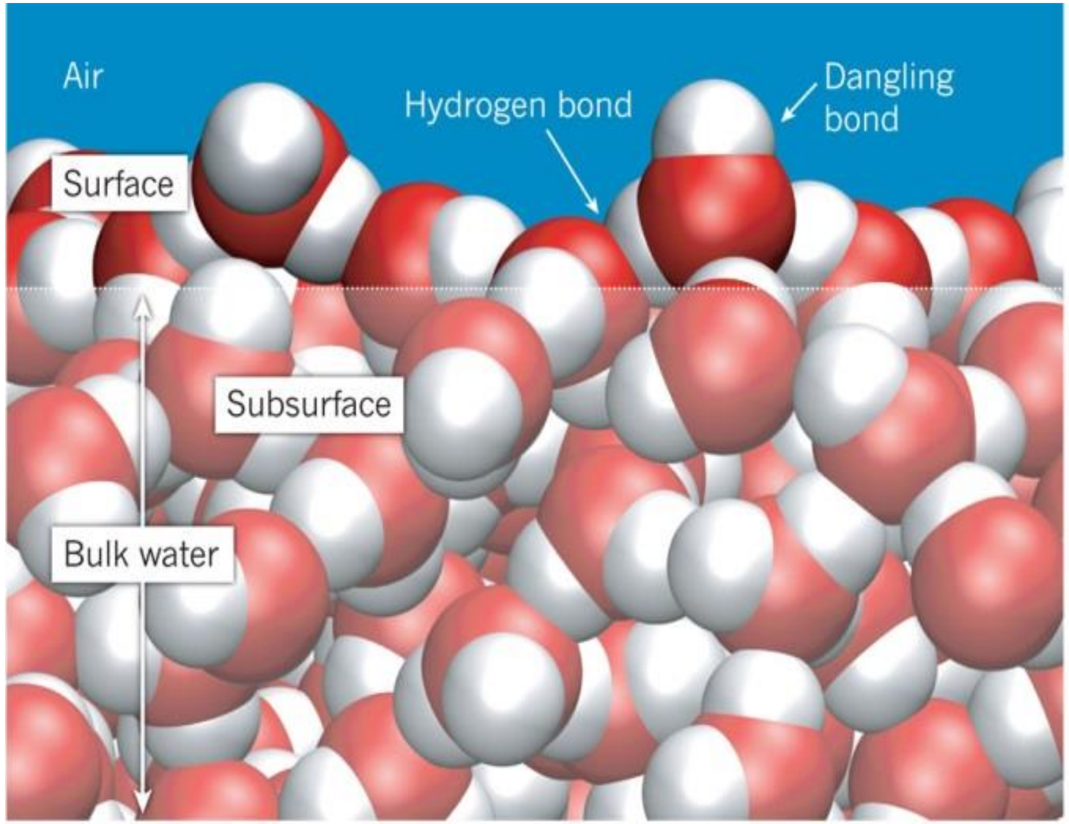

$\chi^{(2)} \neq 0$

Centrosymmetry Broken

$\chi^{(2)} = 0$

SFG with picosecond light pulses → bandwidths narrower than the resonances under investigation.

One of the few attempts to obtain subbandwidth resolution

IR	VIS	SFG
45	60	59
1000	19102	20102

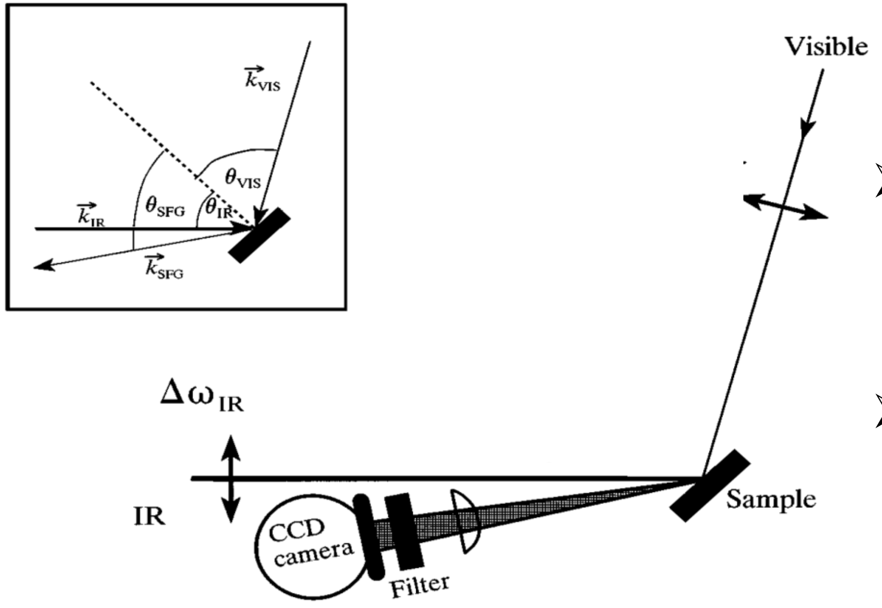

Variation of the SFG exit angle with frequency

- The different frequency components of the sum-frequency (SF) signal can then be collected by different elements of a multielement detector.
- In this case the **spectral resolution depends crucially on the beam divergence.**

$$\omega_{VIS} \sin \theta_{vis} - \omega_{IR} \sin \theta_{IR} = \omega_{SFG} \sin \theta_{SFG}$$

$$\frac{d\theta_{SFG}}{d\omega_{IR}} = -\frac{\omega_{VIS}}{{\omega_{SFG}}^2 \cos \theta_{SFG}}(\sin \theta_{IR} + \sin \theta_{VIS})$$

$$\frac{d\theta_{SFG}}{d\omega_{VIS}} = +\frac{\omega_{IR}}{{\omega_{SFG}}^2 \cos \theta_{SFG}}(\sin \theta_{IR} + \sin \theta_{VIS})$$

At fix θ_{IR} and θ_{VIS}

Another attempt to obtain subbandwidth resolution

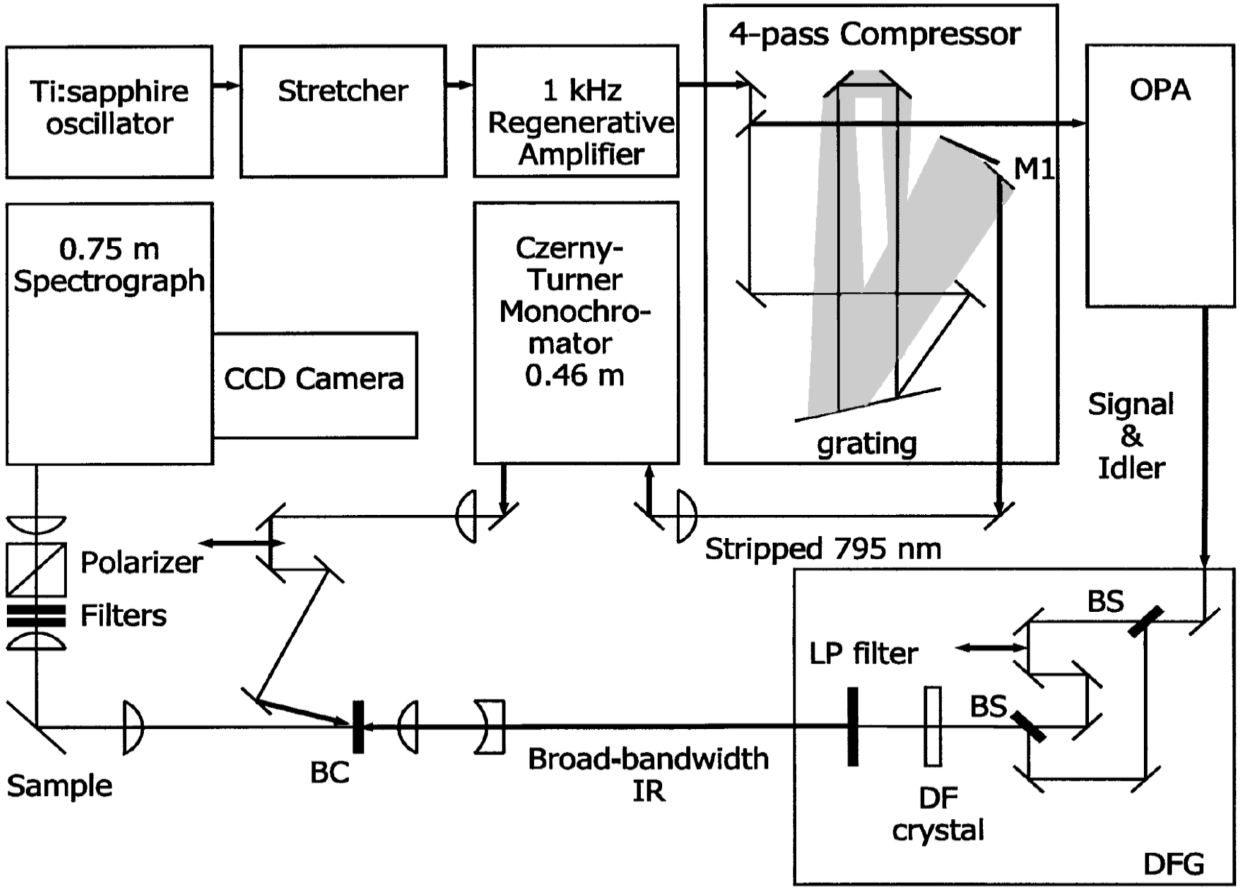

Disperse the broadband SFG signal by a monochromator

- The **spectral resolution depends on** the input pulse characteristics, particularly the **bandwidth of the visible pulse**.

Scheme of Set up and Theory

NEW attempt: Fourier Transform Sum-frequency

Resolution independent on the input pulse characteristic
It is determined by the maximum optical path difference between the two interferometer arms

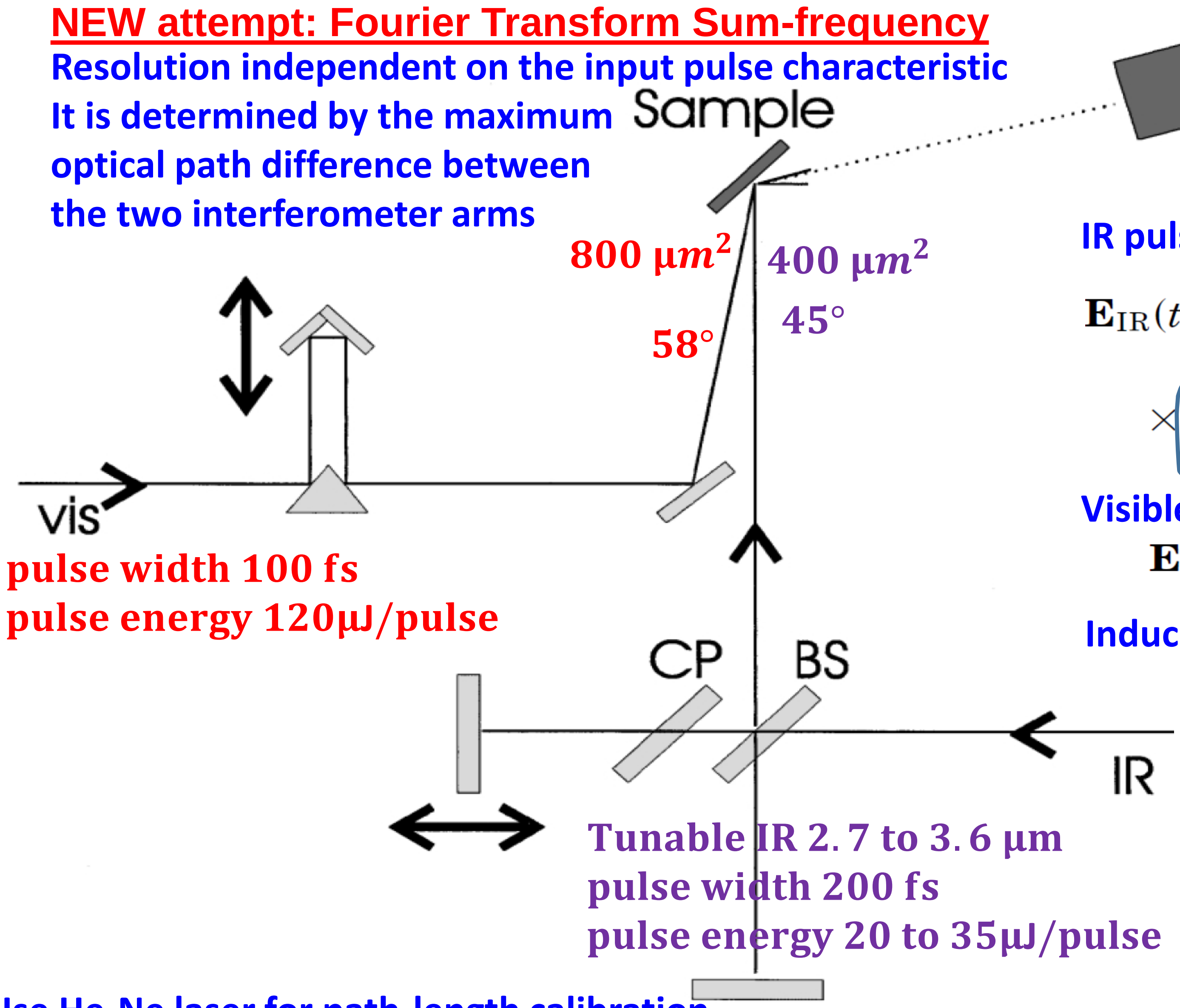

IR pulse Electric Field

$$\mathbf{E}_{\mathrm{IR}}(t-\tau_{\mathrm{IR}}) + \mathbf{E}_{\mathrm{IR}}(t) = \int_{-\infty}^{\infty} \tilde{\mathbf{E}}_{\mathrm{IR}}(\omega_{\mathrm{IR}}) \times \{\exp[-i\omega_{\mathrm{IR}}(t-\tau_{\mathrm{IR}})] + \exp[-i\omega_{\mathrm{IR}}(t)]\}\mathrm{d}\omega_{\mathrm{IR}}\,, \quad (1)$$

Visible pulse Electric Field

$$\mathbf{E}_{V}(t-\tau_{V}) = \int \tilde{\mathbf{E}}_{V}(\omega_{V})\exp[-i\omega_{V}(t-\tau_{V})]\mathrm{d}\omega_{V}$$

Induced nonlinear polarization

$$\mathbf{P}^{(2)}(t,\tau_{\mathrm{iR}},\tau_{V}) = 2\int_{-\infty}^{\infty}\int_{-\infty}^{\infty} \overleftrightarrow{\chi}^{(2)}(\omega=\omega_{V}+\omega_{\mathrm{IR}}) : \tilde{\mathbf{E}}_{V}(\omega_{V})\tilde{\mathbf{E}}_{\mathrm{IR}}(\omega_{\mathrm{IR}})\cos\left(\frac{1}{2}\omega_{\mathrm{IR}}\tau_{\mathrm{IR}}\right)\exp\left[-i\omega_{\mathrm{IR}}\left(t-\frac{\tau_{\mathrm{IR}}}{2}\right)\right] \times \exp[-i\omega_{V}(t-\tau_{V})]\mathrm{d}\omega_{\mathrm{IR}}\mathrm{d}\omega_{V}\,. \quad (2)$$

Use He-Ne laser for path-length calibration

Induced nonlinear polarization

$$\mathbf{P}^{(2)}(t,\tau_{\mathrm{iR}},\tau_V) = 2\int_{-\infty}^{\infty}\int_{-\infty}^{\infty}\overleftrightarrow{\boldsymbol{\chi}}^{(2)}(\omega=\omega_V+\omega_{\mathrm{IR}})$$
$$:\tilde{\mathbf{E}}_V(\omega_V)\tilde{\mathbf{E}}_{\mathrm{IR}}(\omega_{\mathrm{IR}})\cos\left(\frac{1}{2}\,\omega_{\mathrm{IR}}\tau_{\mathrm{IR}}\right)\exp\left[-i\omega_{\mathrm{IR}}\left(t-\frac{\tau_{\mathrm{IR}}}{2}\right)\right]$$
$$\times\exp[-i\omega_V(t-\tau_V)]\mathrm{d}\omega_{\mathrm{IR}}\mathrm{d}\omega_V\,. \quad (2)$$

If the dispersion of $\overleftrightarrow{\boldsymbol{\chi}}^{(2)}$ in ω_V is negligible, we find that

$$\mathbf{P}^{(2)}(t,\tau_{\mathrm{IR}},\tau_V) = 2\int_{-\infty}^{\infty}\overleftrightarrow{\boldsymbol{\chi}}^{(2)}(\omega=\omega_V+\omega_{\mathrm{IR}})$$
$$:\mathbf{E}_V(t-\tau_V)\tilde{\mathbf{E}}_{\mathrm{IR}}(\omega_{\mathrm{IR}})\cos\left(\frac{1}{2}\,\omega_{\mathrm{IR}}\tau_{\mathrm{IR}}\right)$$
$$\times\exp\left[-i\omega_{\mathrm{IR}}\left(t-\frac{\tau_{\mathrm{IR}}}{2}\right)\right]\mathrm{d}\omega_{\mathrm{IR}}\,. \quad (3)$$

For a given set of τ_{IR} and τ_V, the $\hat{i}$-polarized SFG output is proportional to $\int|P_i^{(2)}(t,\tau_{\mathrm{IR}},\tau_V)|^2\mathrm{d}t$. Integration of this output over τ_V yields the desired SFG interferogram:

$$\int\left|P_i^{(2)}(t,\tau_{\mathrm{IR}},\tau_V)\right|^2\mathrm{d}\tau_V$$
$$=4\mathcal{P}_{V,i}\int\left|\chi_{ijk}^{(2)}(\omega=\omega_V+\omega_{\mathrm{IR}})\tilde{E}_{\mathrm{IR},k}(\omega_{\mathrm{IR}})\right|^2$$
$$\times\cos^2\left(\frac{1}{2}\,\omega_{\mathrm{IR}}\tau_{\mathrm{IR}}\right)\mathrm{d}\omega_{\mathrm{IR}}\equiv S(\tau_{\mathrm{IR}})\,, \quad (4)$$

where $\mathcal{P}_{Vj}\equiv\int|E_{V,j}(t-\tau_V)|^2\mathrm{d}\tau_V$.

Fourier Transform of $S(\tau_{\mathrm{IR}})$ give

$$|\chi_{ijk}^{(2)}(\omega=\omega_V+\omega_{\mathrm{IR}})|^2\,|\tilde{E}_{\mathrm{IR},k}(\omega_{\mathrm{IR}})|^2$$

After normalization

$$|\chi_{ijk}^{(2)}(\omega=\omega_V+\omega_{\mathrm{IR}})|^2$$

Experiments

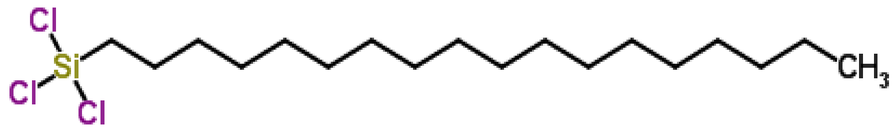

n-octadecyltrichlorosilane [$CH_3CH_{2\,17}SiCl_3$ (OTS)] monolayer on fused silica

Interferograms were obtained by summing five interferograms with τ_V 0, 250, 500, 750, 1000 fs

Maximum IR path difference 1.5 mm spectral resolution is 6.6 cm^{-1}

The spectrum are normalized by the IR pulse spectrum FWHM of 150 cm^{-1}

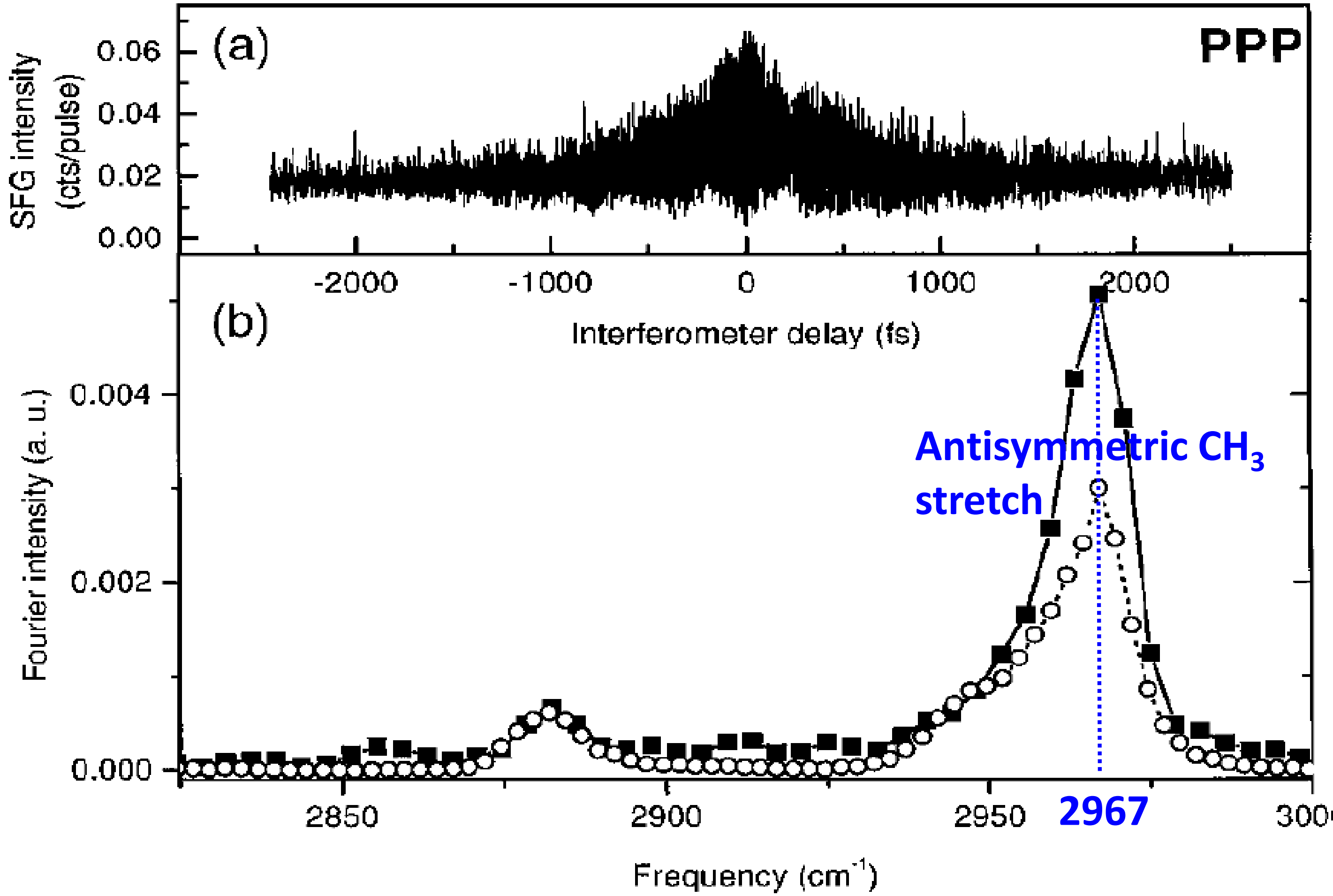

Fig. 2. (a) FT–SFG interferometer trace, along with (b) its FT (squares) and the conventional picosecond SFG spectrum (circles). Polarization configuration, PPP.

spectral resolution is 6 cm^{-1}

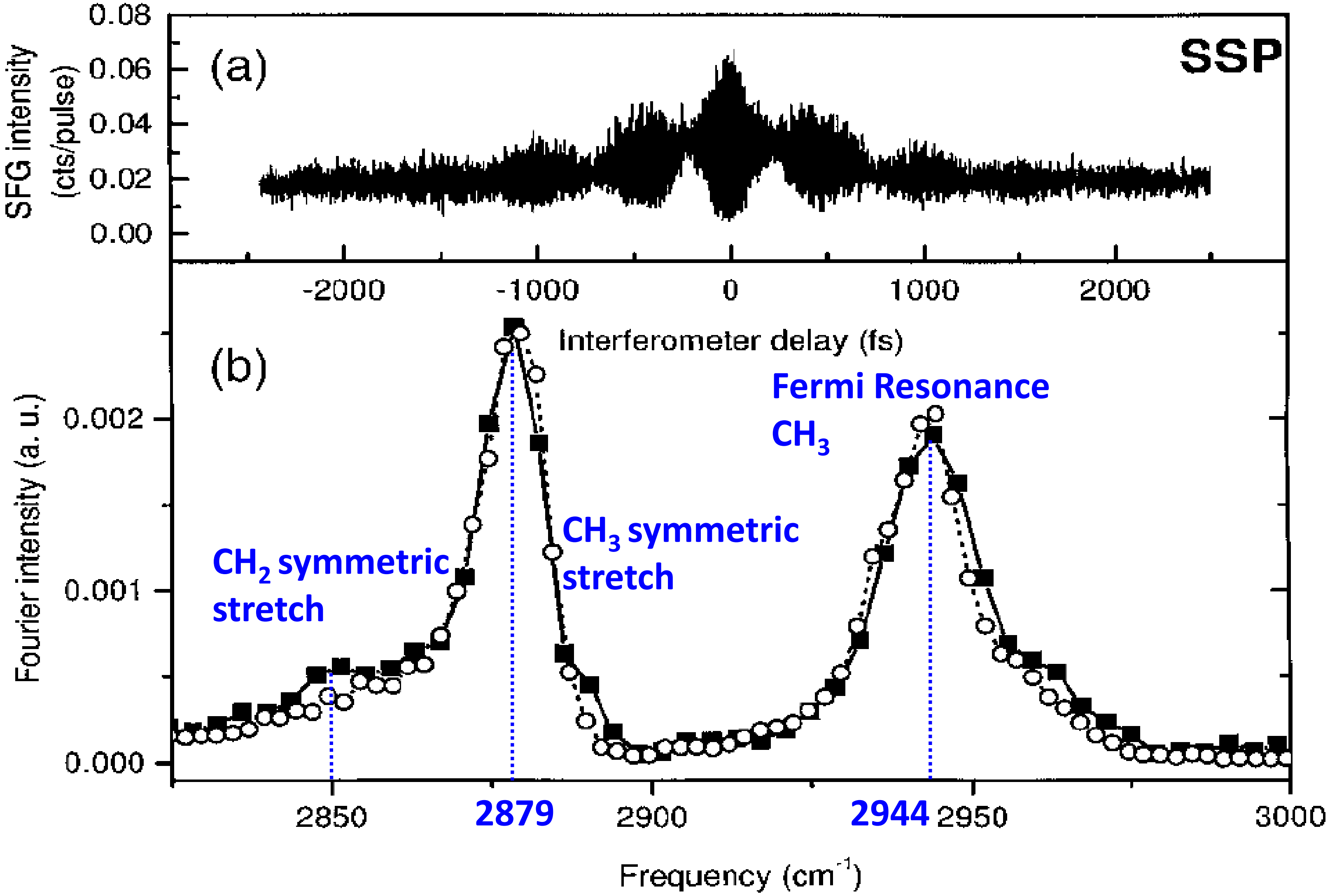

Fig. 3. (a) FT–SFG interferometer trace, along with (b) its FT (squares) and the conventional picosecond SFG spectrum (circles). Polarization configuration, SSP.

The peaks assignment here are more accurate than that in ref6 because of using He-Ne laser for path-length calibration

Main drawback

- Slow scanning speed of IR interferometer
- As in conventional FT spectroscopy, shot noise and source noise in the interferogram should appear as noise over the entire frequency range in the FT spectrum

Conclusion

Main advantages of FT-SFG are

- **The source-independent spectral resolution**
- **The absolute frequency calibration**